Analysing power A_y in the reaction $\vec{p}p \to pp\eta$ close to threshold

P. Winter[1], H.-H. Adam[2], F. Bauer[3], A. Budzanowski[4], R. Czyżykiewicz[5], T. Götz[1], D. Grzonka[1], L. Jarczyk[5], A. Khoukaz[2], K. Kilian[1], C. Kolf[1], P. Kowina[1,6], N. Lang[2], T. Lister[2], P. Moskal[1,5], W. Oelert[1], C. Quentmeier[2], T. Rożek[6], R. Santo[2], G. Schepers[1], T. Sefzick[1], M. Siemaszko[6], J. Smyrski[5], S. Steltenkamp[2], A. Strzałkowski[5], M. Wolke[1], P. Wüstner[7], W. Zipper[6]

[1] *Institut für Kernphysik, Forschungszentrum Jülich, D-52425 Jülich, Germany*

[2] *Institut für Kernphysik, Westfälische Wilhelms–Universität, D - 48149 Münster, Germany*

[3] *I. Institut für Experimentalphysik, Universität Hamburg, D-22761 Hamburg, Germany*

[4] *Institute of Nuclear Physics, PL-31-342 Cracow, Poland*

[5] *Institute of Physics, Jagellonian University, PL-30-059 Cracow, Poland*

[6] *Institute of Physics, University of Silesia, PL-40-007 Katowice, Poland and*

[7] *Zentrallabor für Elektronik, Forschungszentrum Jülich, D-52425 Jülich, Germany*

(Dated: July 10, 2002)

Measurements of the η meson production with a polarised proton beam in the reaction $\vec{p}p \to pp\eta$ have been carried out at an excess energy of $Q = 40\,\mathrm{MeV}$. The dependence of the analysing power A_y on the polar angle θ_q^* of the η meson in the center of mass system (CMS) has been studied. The data indicate the possibility of an influence of p- and d-waves to the close to threshold η production.

PACS numbers: 12.40.Vv, 13.60.Le, 13.88.+e, 24.70.+s, 24.80.+y, 25.10.+s
Keywords: analysing power, polarisation, near threshold meson production, eta

I. INTRODUCTION

Several measurements on the η meson production in the proton-proton interaction covering a 100 MeV excess energy range were performed at different accelerators. The determined total cross sections [1–6], as well as their differential distributions [7–10] triggered intensive theoretical investigations aiming to understand the production mechanism on the hadronic and quark-gluon level.

In the theoretical descriptions of the η-production in nucleon-nucleon collisions the excitation of the $S_{11}(1535)$ resonance plays a decisive role. The hitherto performed studies with the aim to describe the total cross section show a dominance of this virtual S_{11} nucleon isobar in the close-to-threshold production of the η meson. The excitation of this intermediate state results from a one meson exchange (e.g. π, η or ρ) between the two nucleons followed by a strong coupling of the ηN system to the S_{11}.

Near threshold the energy dependence of the total cross section results from a three-body phase space modified by a strong nucleon-nucleon final state interaction and a significant contribution of the attractive interaction in the ηp system. Since several existing models with different scenarios of the excitation describe the existing data well, a confrontation of the predicitions with other observables is needed in order to distinguish between them. The measurements with polarised beam should settle the on-going discussion whether the η production is dominated by ρ [11–14], ω [15] or η [16] exchange. The interference between considered amplitudes causes a different behaviour – depending on the assumed scenario – e.g. of the η meson angular distributions. These differences are too weak in the close-to-threshold region to discriminate between different models. Yet, the predictions of the analysing power depend crucially on the assumed mechanism [17, 18].

So far the only measurement of the analysing power has been performed [8] at an excess energy $Q = 1805\,\mathrm{MeV}$. In the present experiment, the analysing power close to the production threshold is determined and results for the interference terms from contributing partial waves are presented. A comparison with theoretical predictions will be discussed in section V.

Section II contains the description of the experiment and the method to extract the $\vec{p}p \to pp\eta$ events. The following section introduces definitions and gives a theoretical overview. In section IV, the results are presented.

II. EXPERIMENT

Measurements of the $\vec{p}p \to pp\eta$ reaction were performed at the internal experiment COSY-11 [19] at the COoler SYnchrotron COSY [20] in Jülich with a beam momentum of $p_{beam} = 2.096\,\mathrm{GeV/c}$ corresponding to an excess energy of $Q = 40\,\mathrm{MeV}$. During the experiment, cycles of about ten minutes for the two different beam polarisations were adjusted.

Using a hydrogen cluster target [21] in front of one of the regular COSY dipole magnets, the experimental facility acts like a magnetic spectrometer. Positively charged particles in the exit channel are bent towards the interior of the ring where they are detected in a set of two drift chambers. Tracing back the reconstructed trajectories through the magnetic field to the interaction point allows for momentum determination. Particle identification is achieved by a time of flight measurement over a distance of 9.4 m between two scintillation hodoscopes. For further details, the reader is referred to reference [19]. Figure 1(a) shows that the method allows for a clear separation between pions and protons and hence for the identification of events with two protons in the exit channel.

The not registered particle system X – either a single meson (the η in the present case) or a multi meson system – is identified by means of calculating its mass $m_X^2 = (\mathbb{P}_{beam} + \mathbb{P}_{target} - \mathbb{P}_1 - \mathbb{P}_2)^2$, while $\mathbb{P}_{beam}$ and $\mathbb{P}_{target}$ denote the four momentum of the beam and target proton in the initial channel and $\mathbb{P}_1$, $\mathbb{P}_2$ those of the two registered protons. The missing mass spectrum for events with two identified protons is shown in Figure 1(b) for the entire beam time. Besides the clear η-signal there is obviously a π^0-peak resulting from the reaction $\vec{p}p \to pp\pi^0$. Furthermore, a broad yield due to multi pion events with the lower limit given by $m_X^2 = (2m_\pi)^2$ and the upper limit by $m_X^2 = (\sqrt{s} - 2m_p)^2 = 0.345\,\mathrm{GeV^2/c^4}$ is observed. The increasing event rate towards higher missing masses is due to the higher acceptance of the COSY-11 detector for two protons with small momenta in the center of mass system (CMS).

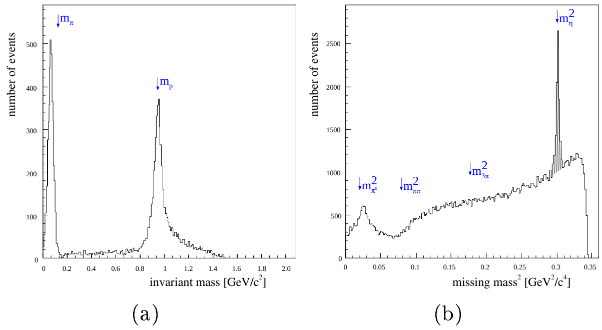

FIG. 1: (a) Invariant mass spectrum for events with two reconstructed tracks. Besides the clear proton peak a second signal stemming from pions is observed. (b) Missing mass squared for events with two protons in the exit channel. Literature values [22] for particle masses are indicated by arrows.

The monitoring of the geometrical dimensions of the synchrotron beam and its position relative to the target [23] enable to achieve a mass resolution of $\sigma_{m_\eta} = 1.6\,\mathrm{MeV/c^2}$. The much broader peak of the π^0 is due to the error propagation which worsens the mass resolution with increasing excess energy [6].

III. GENERAL DESCRIPTION

A. Definitions

A detailed theoretical derivation of the analysing power was recently published for the case of the $\vec{p}\vec{p} \to pp\pi^0$ reaction [24–26]. For the η production the description is analogue since in both measurements the initial channel is fixed to isospin I=1. Therefore, the different quantum numbers for π^0 (as a member of an isotriplet) and the isoscalar η are irrelevant.

In the given experimental situation a convenient choice of the three axis is:

$$\hat{z} = \frac{\vec{p}_{beam}}{|\vec{p}_{beam}|}, \quad \hat{y} = \frac{\vec{P}}{|\vec{P}|} \quad \text{und} \quad \hat{x} = \frac{\vec{y} \times \vec{z}}{|\vec{y} \times \vec{z}|}, \qquad (1)$$

where $\vec{P}$ indicates the polarisation of the COSY beam.

In the COSY-11 experiment, the two four momenta of the final protons $\mathbb{P}_i = (E_i^*, \vec{p}_i^{\,*})$ are measured. The CMS momentum of the η meson is $\vec{q} = -(\vec{p}_1^{\,*} + \vec{p}_2^{\,*})$. The proton momentum in the pp rest-system is denoted by $\vec{p} = \frac{(\vec{p}_1^{\,*} - \vec{p}_2^{\,*})(\vec{p}_1^{\,*} + \vec{p}_2^{\,*})}{2(E_1^* + E_2^*)}$. For later purposes, Figure 2 depicts the definition of the used polar- (θ) and azimuthal angle (φ). The indices p and q will refer to the pp rest-system and of the η meson in the CMS, respectively. The angle θ_p will be choosen such, that $0 \leq \theta_p \leq \pi/2$. This choice guarantees that all observables are invariant under the transformation $\vec{p} \to -\vec{p}$ as required by the identity of the two protons in the final state.

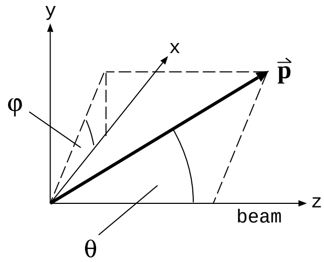

FIG. 2: Definition of the angles. θ is defined as the angle between momentum vector and the z-axis, φ between the x-axis and the projection of $\vec{p}$ onto the x-y-plane.

B. Observables

The differential cross section for a reaction with a polarised beam is given in terms of Cartesian polarisation observables by [27]

$$\sigma(\xi) = \sigma_0(\xi) \left(1 + \sum_{i=1}^{3} P_i \cdot A_i(\xi) \right), \qquad (2)$$

where P_i and A_i denote the beam polarisation and the analysing power in the given reference frame, $\sigma_0(\xi)$ indicates the total cross section in case of no polarisation. In the upper formula, the abbreviation

$$\sigma(\xi) = \frac{d^3\sigma}{d\Omega_p d\Omega_q dE_{pp}}(\xi)$$

is used where ξ denotes the set of the five variables which are kinematically completely describing the exit channel, namely (θ_p, φ_p, θ_q^*, φ_q^*, E_{pp}). The kinetic energy E_{pp} of the two final protons in their CM system is given by $E_{pp} = \sqrt{s_{12}} - 2m_p$ with $\sqrt{s_{12}} = 2\sqrt{\vec{p}^{\,2} + m_p^2}$ as the energy in the pp subsystem.

In the given case of the general experimental conditions, the beam polarisation is – due to the magnetic fields in the accelerator – forced to be $\vec{P} = (0, P_y, 0)^T$ and hence formula (2) simplifies to

$$\sigma(\xi) = \sigma_0(\xi)\big(1 + P_y \cdot A_y(\xi)\big). \tag{3}$$

The asymmetry ε – obtained from the difference in the yields with beam polarisation up and down – defined by

$$\varepsilon := \frac{N_\uparrow - N_\downarrow}{N_\uparrow + N_\downarrow} \tag{4}$$

forms the basis for deducing the analysing power while $N_\uparrow$ ($N_\downarrow$) denote the experimental number of events for spin up (down). With known luminosity $\mathcal{L}$, efficiency $\mathcal{E}$ and measured time dt, dN is related to the cross section by $dN_{\uparrow,\downarrow} = \mathcal{E} \cdot \mathcal{L} \cdot \sigma_{\uparrow,\downarrow} \cdot dt$. In combination with equation (3), one can deduce from (4) that

$$A_y(\xi) = \frac{\mathcal{L}_{rel} \cdot N_\uparrow - N_\downarrow}{N_\downarrow \cdot P_\uparrow - \mathcal{L}_{rel} \cdot P_\downarrow \cdot N_\uparrow}(\xi), \tag{5}$$

where the relative time-integrated luminosity $\mathcal{L}_{rel}$ is defined by $\mathcal{L}_{rel} := \frac{\int \mathcal{L}_\downarrow \cdot dt_\downarrow}{\int \mathcal{L}_\uparrow \cdot dt_\uparrow}$. In equation (5), the efficiency cancels out because of the independence on the spin as long as the bin size of $\Delta\xi$ is small enough so that the efficiency can be assumed to be constant.

With the definitions given in section III A, the angular dependence of the spin-dependent cross section can be written as [24]:

$$\begin{aligned}
\sigma_0(\xi)A_y(\xi) \;=\; & \Big\{\big[G_1^{y0} + G_2^{y0}(3\cos^2\theta_p - 1)\big]\sin\theta_q^* + \big[H_1^{y0} + I^{y0} + H_2^{y0}(3\cos^2\theta_p - 1)\big]\sin 2\theta_q^*\Big\}\cos\varphi_q^* \\
& + \big[H_3^{y0} + K^{y0} + G_3^{y0}\cos\theta_q^* + H_4^{y0}(3\cos^2\theta_q^* - 1)\big]\sin 2\theta_p \cos\varphi_p \\
& + (G_4^{y0}\sin\theta_q^* + H_5^{y0}\sin 2\theta_q^*)\sin^2\theta_p\cos(2\varphi_p - \varphi_q^*) + H_6^{y0}\sin 2\theta_p \sin^2\theta_q^*\cos(2\varphi_q^* - \varphi_p)
\end{aligned} \tag{6}$$

The appearing literals[1] denote interferences of partial wave amplitudes. The relative angular momentum of the two outgoing protons in their rest system is denoted by capital letters $l_p = S, P, D \ldots$, the one of the η meson in the CMS by small letters $l_q = s, p, d \ldots$, while the usual spectroscopic notation is used. With this definition, the single terms $G_k^{y0}, H_k^{y0}, I^{y0}$ and K^{y0} correspond to (PsPp), $(\mathrm{Pp})^2$, (SsSd) und (SsDs).

IV. RESULTS

In order to extract the assymetry from the measured spinup and spindown events one needs the relative luminosity and the average beam polarisation.

Via a simultaneous measurement of the proton-proton elastic scattering at the internal experiment EDDA [28, 29] the polarisation was determined for two time blocks[2]:

	time block 1	time block 2
$P_\uparrow$	0.381 ± 0.007	0.497 ± 0.006
$P_\downarrow$	-0.498 ± 0.007	-0.572 ± 0.007

The relative luminosity $\mathcal{L}_{rel} = \frac{N_\downarrow^{elas}}{\sigma_\downarrow^{elas}} \cdot \frac{\sigma_\uparrow^{elas}}{N_\uparrow^{elas}}$ was extracted via the elastic proton-proton scattering. To determine the elastic cross $\sigma_{\uparrow,\downarrow}^{elas}$ section according to equation (3) the analysing power was taken from [30]. With the number of events $N_{\uparrow,\downarrow}^{elas}$ resulting from the elastic pp scattering $\mathcal{L}_{rel}$ was calculated according to the definition given above:

	time block1	time block 2
$\mathcal{L}_{rel}$	$1.004 \pm 0.004\,^{+0.002}_{-0.002}$	$0.949 \pm 0.004\,^{+0.001}_{-0.001}$

An integration of equation (6) over $\cos\theta_p$ and φ_p leads to the disappearance of several terms provided the experimental angular distribution covers either the full phase space with a constant detector efficiency or symmetrical ranges. Figure 3 shows the angular distributions of $pp\eta$-events from a Monte-Carlo simulation which are neither constant nor symmetric arround 0 and 90° in case of $\cos\theta_p$ and φ_p, respectively. Therefore, the evaluation of the analysing power requires an efficiency correction. To correct the data the efficiency $\mathcal{E}(\cos\theta_p, \varphi_p)$ is determined via Monte-Carlo simulations. Using a GEANT-3 code for each event a detection system response was calculated and the simulated data sample was analysed with the same programme which is used for the analysis of the experimental data. Weights $w(\cos\theta_p, \varphi_p) = 1/\mathcal{E}(\cos\theta_p, \varphi_p)$ were applied during the final analysis of the experimental

[1] The superscript $y0$ indicates a beam polarisation along the y-axis and an unpolarised target.

[2] The significant increase of the polarisation from the first to the second block is caused by a development of the polarisation in between.

data and hence the corrected number of events reads:

$$N^{cor} = \frac{\sum\limits_i \sum\limits_k w_{i,k} N_{i,k}}{\sum\limits_i \sum\limits_k w_{i,k}}\,, \tag{7}$$

while i and k run over the bins φ_p and $\cos\theta_p$, respectively. The error is deduced with $\Delta N_{i,k} = \sqrt{N_{i,k}}$ to be

$$\Delta N^{cor} = \frac{1}{\sum\limits_i \sum\limits_k w_{i,k}} \sqrt{\sum_i \sum_k w_{i,k}^2 N_{i,k}}\,,$$

whereas the error of $w_{i,k}$ was neglected because of a much higher statistic for the Monte Carlo simulations, so that $\frac{\Delta w_{i,k}}{w_{i,k}} \ll \frac{\Delta N_{i,k}}{N_{i,k}}$. The influence of the strong proton-proton final state-interaction (FSI) was included via the description with a Jost-function [31]. Former acceptance studies on the dependence on the various Jost function prescriptions showed a change of the result of maximum 10% [32, 33]. Concerning that the FSI is known up to a accuracy of around 30% one can conclude that the upper limit for the total contribution to the error is approximately 3% which is negligible compared to the high overall error of this first data sample.

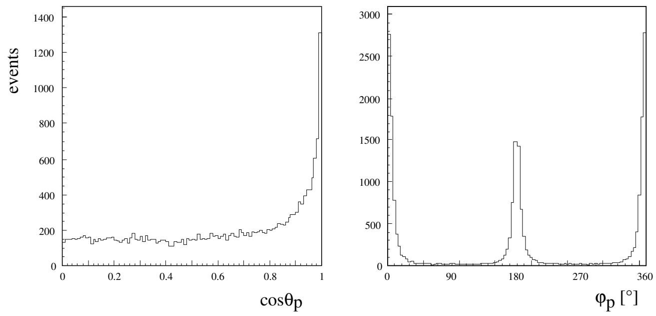

FIG. 3: Angular distribution for the two proton angles $\cos\theta_p$ and φ_p obtained via Monte-Carlo simulations.

Only after an efficiency correction one can remove the dependency from proton-coordinates in the analysis which is then the same as an integration over these variables so that equation (6) simplifies to:

$$\iint \frac{d^2\sigma}{d\Omega_p d\Omega_q}(\xi)\, A_y(\xi)\, d\cos\theta_p\, d\varphi_p = 2\pi \left(G_1^{y0} \sin\theta_q^* + (H_1^{y0} + I^{y0}) \sin 2\theta_q^*\right) \cos\varphi_q^*. \tag{8}$$

Due to the restricting dipole gap φ_q^* is dominantly peaked around 0° – quite similar to the φ_p distribution – but with a negligible peak around 180° which is not shown here but verified with MC simulations. Therefore, the analysis was performed with one single φ_q^*-bin around ±30°. Hence, equation (8) leads further to the separation of the (PpPs)-interference (G_1^{y0}) and the (Pp)^2- and (SsSd)-terms (H_1^{y0} and I^{y0}):

$$\begin{aligned} G_1^{y0} &= \frac{1}{\pi^2} \int f(\cos\theta_q^*)\, d\cos\theta_q^*\,, \\ H_1^{y0} + I^{y0} &= \frac{2}{\pi^2} \int f(\cos\theta_q^*) \cos\theta_q^*\, d\cos\theta_q^*\,, \end{aligned} \tag{9}$$

with $f(\cos\theta_q^*) = \int\limits_{-\frac{\pi}{6}}^{\frac{\pi}{6}} \int\limits_0^{2\pi} \int\limits_0^1 \frac{d^2\sigma}{d\Omega_p d\Omega_q}(\xi)\, A_y(\xi)\, d\cos\theta_p d\varphi_p d\varphi_q^*$.

Defining[3] $\bar{N}(\cos\theta_q^*) := \iiint N^{cor.}(\xi)\, d\Omega_p\, d\varphi_q^*$, it is straightforward to show analogue to equations (4) and (5) that the integrated analysing power defined by

$$\bar{A}_y(\cos\theta_q^*) := f(\cos\theta_q^*) / \frac{d\sigma}{d\cos\theta_q^*} \tag{10}$$

can be determined via

$$\bar{A}_y(\cos\theta_q^*) = \frac{\mathcal{L}_{rel} \cdot \bar{N}_{\eta,\uparrow} - \bar{N}_{\eta,\downarrow}}{P_\uparrow \cdot \bar{N}_{\eta,\downarrow} - \mathcal{L}_{rel} \cdot P_\downarrow \cdot \bar{N}_{\eta,\uparrow}}(\cos\theta_q^*). \tag{11}$$

The calculation of $\bar{A}_y$ needs the determination of the absolute $\vec{p}p \to pp\eta$ events $\bar{N}_{\eta,\uparrow\downarrow}$ in dependence of $\cos\theta_q^*$. In section II, the selection of the ppη was discussed. The analysis was performed with 4 bins in $\cos\theta_q^*$ starting at $\cos\theta_q^* = -0.75$ with $\Delta\cos\theta_q^* = 0.5$. A representative missing mass spectrum is shown in Figure 4(a) where the background is fitted by a polynomial function. From this spectrum the number of events $\bar{N}_{\eta+b}$ including background and η-event are extracted. Subsequently, this background is substracted and the number of events $\bar{N}_\eta$ are determined (Figure 4(b)).

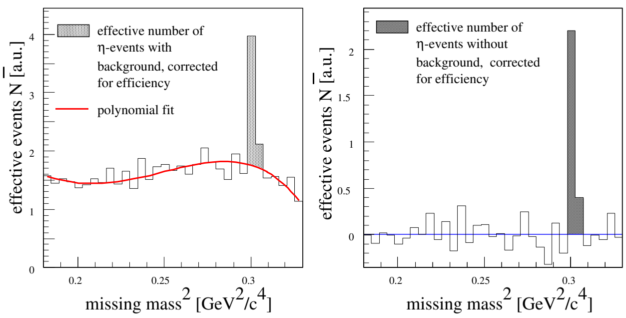

(a) (b)

FIG. 4: Spectra of the squared missing mass for events with two identified protons (a) with and (b) after substraction of the background. The number of events was corrected according to equation (7).

For the two time blocks, an error weighted mean value for $\bar{A}_y$ is calculated. Figure 5 shows the analysing power

[3] In the following, limits of the integrations will be omitted as they are always the same.

as a function of $\cos\theta_q^*$. The extraction of G_1^{y0} and $H_1^{y0} + I^{y0}$ with equations (9) needs according to (10) the knowledge of $\frac{d\sigma}{d\cos\theta_q^*}$ which was taken from [7]. The fact that $\varphi_q \in [-\frac{\pi}{6}, \frac{\pi}{6}]$ was considered with $\frac{d\sigma}{d\cos\theta_q^*} = \int_{\frac{\pi}{6}}^{-\frac{\pi}{6}} \frac{d\sigma}{d\Omega_q^*}\, d\varphi_q^*$ which is due to the isotropy of the cross section in φ

$$\left.\frac{d\sigma}{d\cos\theta_q^*}\right|_{-\frac{\pi}{6}\le\varphi_q^*\le\frac{\pi}{6}} = \frac{\pi}{3}\frac{d\sigma}{d\Omega_q^*}. \qquad (12)$$

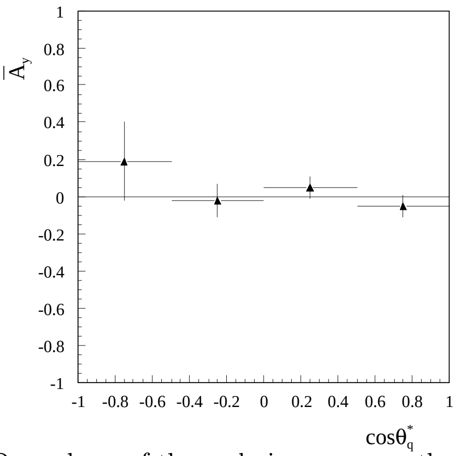

FIG. 5: Dependence of the analysing power on the center of mass polar angle θ_q^* of the η meson.

The averaged values of $\bar{A}_y$ and the cross section used for the integrations in equations (9) are presented in table I.

$\cos\theta_q$	$\bar{A}_y$	$\frac{d\sigma}{d\cos\theta_q}$ [μb]
-0.75 ± 0.25	0.27 ± 0.21	0.31 ± 0.01
-0.25 ± 0.25	0.06 ± 0.09	0.50 ± 0.01
0.25 ± 0.25	0.05 ± 0.06	0.50 ± 0.01
0.75 ± 0.25	-0.05 ± 0.06	0.31 ± 0.01

TABLE I: Analysing power as a function of the emission angle θ_q of the η meson in the CMS and the differential cross section obtained from [7] with equation (12).

Finally, the integrations of these values

$$G_1^{y0} = \frac{1}{\pi^2}\sum_{\cos\theta_q^*}\frac{d\sigma}{d\cos\theta_q^*}\bar{A}_y\cdot\Delta\cos\theta_q^*$$

$$H_1^{y0} + I^{y0} = \frac{2}{\pi^2}\sum_{\cos\theta_q^*}\frac{d\sigma}{d\cos\theta_q^*}\bar{A}_y\cos\theta_q^*\cdot\Delta\cos\theta_q^*.$$

result in

$$G_1^{y0} = (0.003 \pm 0.004)\,\mu\text{b}$$

and

$$H_1^{y0} + I^{y0} = (-0.005 \pm 0.005)\,\mu\text{b}.$$

V. COMPARISON WITH THEORY

The present data on the η meson production in nucleon-nucleon collisions referred to in section I show not only the 3-body phase space Q^2-dependency and a modification due to the nucleon-nucleon final state interaction but also a significant influence of the nucleon-meson interaction in the case of the ηp system. As mentioned above, several models describe the existing data quite well although they are based on different assumptions for the excitation mechanism of the S_{11} resonance. For instance, Batinić et al. [16] or Nakayama, Speth and Lee [18] found a dominance of π and η-exchange in the analysis of $pp \to pp\eta$ while Fäldt and Wilkin [17] conclude a dominant ρ-exchange.

Polarisation observables may be the right tool to distinguish between the different models. Calculations for the analysing power in the reaction $\vec{p}p \to pp\eta$ show different results depending on the underlying assumption for the one meson exchange model. Figure 6 presents results taken from references [17] (dotted line) and [18] (solid and dashed lines) for $Q = 10\,$MeV and 37 MeV. The authors of the latter reference conclude in the full model calculations a dominance of π and η-exchange (solid line). The dashed curve represents a vector dominance model with an exclusion of π and η-exchange for exciting the S_{11} resonance. The triangles are the experimental results.

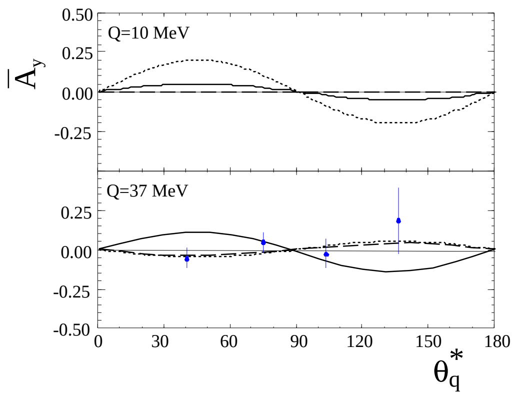

FIG. 6: Analysing power for the reaction $\vec{p}p \to pp\eta$ in dependence on θ_q^* for the two excess energies $Q = 10\,$MeV and 37 MeV.

The observable structure of the experimental values show a slight deviation from the $\sin\theta_q\cos\theta_q$-dependence of both models. Especially, the full model calculations of Nakayama, Speth and Lee [18] seem to disagree with the data. The more or less strong difference in the angular dependency of A_y results from a vanishing G_1^{y0} in both references. As this corresponds to the (PpPs)-term, an influence of the P-wave must be suspected. Therefore, H_1^{y0} – describing the (Pp)^2 interference – should have a non negligible contribution, too. For further detailed studies the data are not yet precise enough to disentangle the sum of H_1^{y0} and I^{y0}.

VI. CONCLUSION

The reaction $\vec{p}p \to pp\eta$ has been studied at an excess energy of $Q = 40\,\mathrm{MeV}$. The final state has been kinematically completely reconstructed and the analysing power has been determined. Qualitatively, the data seem to favour the calculations with dominant vector meson exchange but definitive conclusions cannot be drawn due to the large uncertainties of the data. To allow a more rigorous comparison with theoretical calculations higher statistics experiments are required and already scheduled for 2002 at COSY-11.

VII. ACKNOWLEDGEMENTS

We are very grateful for the support of the EDDA-collaboation in determing the beam polarisation. Furthermore, we would like to thank C. Wilkin, C. Hanhart and K. Nakayama for very helpful discussions and contributions.

Our special thanks go to Prof. Dr. J. Treusch, chairman of the board of directors of the research center Jülich, for undertaking a nightshift during the experiment.

This work has been supported by the International Büro and the Verbundforschung of the BMBF, the Polish State Committee for Scientific Research, the FFE grants from the Forschungszentrum Jülich, the Forschungszentrum Jülich directorates and the European Community - Access to Research Infrastructure action of the Improving Human Potential Programme.

[1] A. M. Bergdolt et al., Phys. Rev. **D 48**, 2969 (1993).
[2] E. Chiavassa et al., Phys. Lett. **B 322**, 270 (1994).
[3] H. Calén et al., Phys. Lett. **B 366**, 39 (1996).
[4] H. Calén et al., Phys. Rev. Lett. **79**, 2642 (1997).
[5] F. Hibou et al., Phys. Lett. **B 438**, 41 (1998).
[6] J. Smyrski et al., Phys. Lett. **B 474**, 182 (2000).
[7] H. Calén et al., Phys. Lett. **B 458**, 190 (1999).
[8] B. Tatischeff et al., Phys. Rev. **C 62**, 054001 (2000).
[9] P. Moskal et al., πN Newsletter **16**, 367 (2002).
[10] M. Abdel-Bary et al. (2002), e-Print Archive: nucl-ex/0205016.
[11] J. F. Germond and C. Wilkin, Nucl. Phys. **A 518**, 308 (1990).
[12] J. M. Laget, F. Wellers, and J. F. Lecolley, Phys. Lett. **B 257**, 254 (1991).
[13] A. B. Santra and B. K. Jain, Nucl. Phys. **A 634**, 309 (1998).
[14] E. Gedalin, A. Moalem, and L. Razdolskaja, Nucl. Phys. **A 634**, 368 (1998).
[15] T. Vetter, A. Engel, T. Biro, and U. Mosel, Phys. Lett. **B 263**, 153 (1991).
[16] M. Batinić, A. Svarc, and T. S. H. Lee, Phys. Scripta **56**, 321 (1997).
[17] G. Fäldt and C. Wilkin, Phys. Scripta **64**, 427 (2001).
[18] K. Nakayama, J. Speth, and T. S. H. Lee, Phys. Rev. **C 65**, 045210 (2002).
[19] S. Brauksiepe et al., Nucl. Instr. & Meth. **A 376**, 397 (1996).
[20] R. Maier, Nucl. Instr. & Meth. **A 390**, 1 (1997).
[21] H. Dombrowski et al., Nucl. Instr. & Meth. **A 386**, 228 (1997).
[22] D. E. Groom et al., Eur. Phys. J. **C 15**, 1 (2000).
[23] P. Moskal et al., Nucl. Instr. & Meth. **A 466**, 444 (2001).
[24] H. O. Meyer et al., Phys. Rev. **C 63**, 064002 (2001).
[25] H. O. Meyer et al., Phys. Rev. Lett. **83**, 5439 (1999).
[26] H. O. Meyer et al., Phys. Rev. Lett. **81**, 3096 (1998).
[27] D. Fick, *Einführung in die Kernphysik mit polarisierten Teilchen* (Bibliographisches Institut, Mannheim, 1971).
[28] J. Bisplinghoff et al., Nucl. Instr. & Meth. **A 329**, 151 (1993).
[29] M. Altmeier et al., Nucl. Instr. & Meth. **A 431**, 428 (1999).
[30] M. Altmeier et al., Phys. Rev. Lett. **85**, 1819 (2000).
[31] M. L. Goldberger and K. M. Watson, *Collision theory*, Structure of matter series (John Wiley & Sons, Inc., New York, 1964).
[32] P. Moskal et al., Phys. Lett. **B 482**, 356 (2000).
[33] P. Moskal et al., Phys. Lett. **B 474**, 416 (2000).